Letter

Theory of magnetic excitations in the multilayer nickelate superconductor $La_3Ni_2O_7$

Steffen Bötzel,* Frank Lechermann, Jannik Gondolf, and Ilya M. Eremin
Theoretische Physik III, Ruhr-Universität Bochum, D-44780 Bochum, Germany

(Received 29 January 2024; revised 19 March 2024; accepted 12 April 2024; published 6 May 2024)

Motivated by the recent reports of high-T_c superconductivity in $La_3Ni_2O_7$ under pressure, we analyzed theoretically the magnetic excitations in the normal and the superconducting state in this compound, which can be measured by inelastic neutron scattering or resonant inelastic x-ray scattering. We show that the bilayer structure of the spin response allows us to elucidate the role of the interlayer interaction and the nature of the Cooper pairing in a very efficient way. In particular, we demonstrate the key difference between the potential $s_{\pm}$- and d-wave gaps, proposed recently, by comparing the corresponding response in the even and odd channels of the spin susceptibility. We show that the mostly interlayer driven bonding-antibonding $s_{\pm}$ Cooper pairing produces a single large spin resonance peak in the odd channel only near the X point, whereas spin resonances in both the odd and the even channel are predicted for the d-wave scenario.

DOI: 10.1103/PhysRevB.109.L180502

Introduction. The discovery of unconventional superconductivity in hole-doped thin films of infinite-layer and reduced multilayer nickelates [1–3] has stimulated further interest in studying exotic quantum states and potential superconductivity in the so-called Ruddlesden-Popper (RP) series of the nickel-based oxides, denoted as $R_{n+1}Ni_nO_{3n+1}$, where R refers to a rare-earth element and n is the number of consecutive layers. The most recent breakthrough in this direction are reports of high-pressure superconductivity around 80 K in $La_3Ni_2O_7$ [4–11] and around 20 K in $La_4Ni_3O_{10}$ [12–15]. These exciting discoveries have motivated massive theoretical investigation [16–54], yet the full structural characterization of these systems is still under debate [7,55,56]. Nevertheless, a striking increase of the superconducting transition temperature in $La_3Ni_2O_7$ with multilayer or bilayer structure calls for a careful theoretical examination.

Considering $La_3Ni_2O_7$ as a RP bilayer system yields a formal Ni $3d^{7.5}$ (or $3d^8$ when considering ligand-hole physics [16]) electronic configuration with both Ni e_g orbitals crossing the Fermi level. The low-energy physics in this system is ruled by the multiorbital and the bilayer effects with strong hybridization between the Ni d_{z^2} orbitals and the apical O-p_z orbitals [40]. The multiorbital structure seems to be one of the key differences between $La_3Ni_2O_7$ and the bilayer cuprate superconductors where Cu^{2+} ions with a $3d^9$ configuration possess only one unpaired valence electron in the $3d_{x^2-y^2}$ orbital, whereas the Ni ion has unpaired valence electrons in both the $3d_{x^2-y^2}$ and $3d_{z^2}$ orbitals. Various Hubbard-Hund-type or t-J like models have already been proposed to capture the superconducting and normal state properties of this multiorbital system [16–22,28–37].

Within the variety of model considerations, one of the most interesting theoretical question concerns the interplay between the intralayer and the interlayer Cooper pairing [57], which yields a competition between the $s_{\pm}$-wave symmetry of the superconducting order parameter, driven mostly by the interlayer Cooper pairing [16–27,54] and the $d_{x^2-y^2}$-wave or the d_{xy}-wave symmetries of the superconducting order parameters, driven mostly by the intralayer interaction, respectively [16,17,27,28,46].

Given the likely nonphononic origin of superconductivity in pressurized $La_3Ni_2O_7$, the strange metal behavior of the normal state [4,6,10], and the signatures of magnetic ordering, seen at the ambient pressure [58,59] at around 150 K, it is instructive to study the bilayer-structure impact on the spin response in this system in the normal and superconducting states. Recall that one of the important hallmarks of the superconducting state in unconventional superconductors is the occurrence of the so-called spin resonance. It is seen by the inelastic neutron scattering in various systems at the antiferromagnetic (AFM) wave vector $\mathbf{Q}_{\mathrm{AFM}} = (\pi, \pi)$ at energies below or around the superconducting gap energy threshold of about 2Δ [60]. Its presence in various unconventional superconductors ranging from high-T_c cuprates [61–65], iron-based superconductors [66–69], and some heavy-fermion superconductors like $CeCoIn_5$ [70,71] is considered to be one of the strong signatures of spin-fluctuation-mediated Cooper pairing [60,72]. In the simplest theoretical picture, the spin resonance peak occurs due to a change of sign of the superconducting order parameter at the parts of the Fermi surface which are connected by the AFM wave vectors $\Delta_{\mathbf{k}}$ and $\Delta_{\mathbf{k+Q}}$ [73–81].

The occurrence of the resonance peaks and their dispersion in bilayer systems not only allows one to confirm the unconventional nature of superconductivity and to learn about the superconducting gap symmetry but also allows one to understand the importance of the interlayer coupling. In particular, due to two CuO_2 layers per unit cell, the spin response in bilayer cuprates splits into even and odd channels. This in turn can be connected to the bonding and antibonding character of the electronic bands, showing modulations in q_z directions [82]. The magnetic susceptibility splits into even χ_e and odd χ_o susceptibilities [83–86] and they can be accessed individually by measuring the spin response at different q_z momenta.

*Corresponding author: Steffen.Boetzel@ruhr-uni-bochum.de

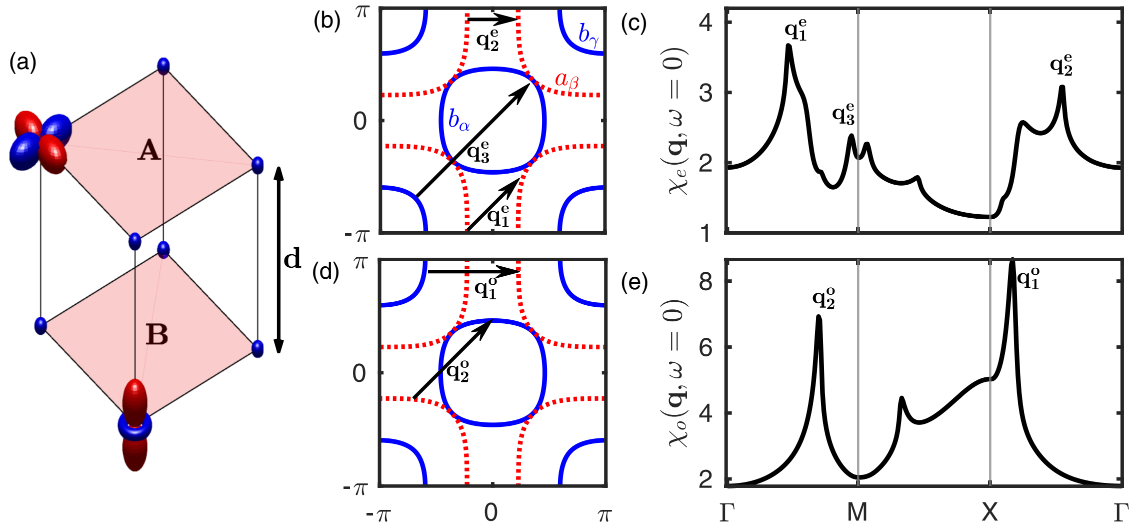

FIG. 1. (a) Schematic representation of the bilayer model with e_g orbitals. Panels (b) and (d) show the Fermi surface for the model [33] with bonding (b) and antibonding (a) bands shown by blue (solid) and red (dashed) curves, respectively. Note the sign-changing bonding-antibonding $s_\pm$ gap follows the same red-blue color distribution referring to the negative and positive regions of the gap. Greek indices denote the notion of the bands, accepted in literature. The arrows in panels (b) and (d) highlight the important scattering wave vectors in the even and odd channels, respectively. Panels (c) and (e) show the even (χ_e) and the odd (χ_o) parts of the static RPA susceptibility in arbitrary units, respectively, calculated in the normal state ($T = 80$ K) for $U = 0.9U_{\mathrm{mag}}$ and $J_{\mathrm{H}} = U/7$. Peaks are labeled according to scattering vectors displayed in panels (b) and (d).

In bilayer cuprates, the spin resonance peak was found in both channels in a wide doping range with clear splitting between χ_e and χ_o [87,88]. Furthermore, analyzing their intensities and frequency positions, one was able to extract important information of the overall structure of the paramagnon continuum and the interplay of interlayer exchange interactions and interlayer hopping matrix elements [83–86]. In $La_3Ni_2O_7$ the situation is even more intriguing, because the splitting of bonding and antibonding bands is much stronger.

In this work, we provide a theoretical description of the spin response of paramagnetic $La_3Ni_2O_7$ in the pressurized normal and superconducting state. We begin by considering the spin response in multiorbital bilayer systems and then focus on two different scenarios for the superconducting pairing. First, we consider $s_\pm$ interlayer pairing with a sign change between bonding and antibonding bands. Using the tight-binding model from Ref. [33] we discuss the important scattering vectors contributing to χ_e and χ_o. We find that χ_o gives a much larger spin response. In the superconducting state, this scenario manifests in a dominant spin resonance peak near the X point. The second scenario is a cupratelike $d_{x^2-y^2}$ gap symmetry which is discussed in the context of the model presented in Ref. [16]. Here, the spin response for χ_e and χ_o channels is of the same order. Correspondingly, this scenario yields different spin resonance peaks in the superconducting state in both χ_e and χ_o. Measuring the spin response in both channels can, therefore, clearly reveal the actual Cooper-pairing scenario and clarify the role of the interlayer exchange interaction in this system.

Theoretical approach. We consider an effective quasi-two-dimensional bilayer Hamiltonian for the Ni e_g orbitals, illustrated in Fig. 1(a), which follows from the tight-binding models developed previously [16,33]. The considered Hamiltonian consists of noninteracting and multiorbital on-site interacting parts $\mathcal{H} = \mathcal{H}_0 + \mathcal{H}_{\mathrm{int}}$. Note that the combination of the large interlayer hopping of the system and the on-site interaction results in an effective interlayer interaction corresponding to the superexchange process through the inner apical oxygen.

In momentum space the noninteracting part reads

$$\mathcal{H}_0 = \sum_{\mathbf{k},k_z} \sum_{l_1,l_2} \sum_{o_1,o_2} \hat{H}_{l_1o_1;l_2o_2}(\mathbf{k}, k_z) c^\dagger_{l_1o_1}(\mathbf{k}, k_z) c_{l_2o_2}(\mathbf{k}, k_z), \quad (1)$$

where $c^\dagger_{l,o}(\mathbf{k}, k_z)$ creates an electron in layer l and orbital o with in-plane momentum $\mathbf{k} = (k_x, k_y)$. In our modeling, the out-of-plane momentum k_z only enters in the phase factors arising from the Fourier transform for a bilayer system. We denote the upper and the lower layer with A and B, respectively. As the Hamiltonian must be invariant under exchange of layers, we find $\hat{H}_{AA} = \hat{H}_{BB} = \hat{H}_\parallel$ and $\hat{H}_{AB} = \hat{H}_{BA} = \hat{H}_\perp$ for the intralayer and interlayer hoppings, respectively, yielding the general form

$$\hat{H}(\mathbf{k}, k_z) = \begin{pmatrix} \hat{H}_\parallel(\mathbf{k}) & \hat{H}_\perp(\mathbf{k}) e^{ik_zd} \\ \hat{H}_\perp(\mathbf{k}) e^{-ik_zd} & \hat{H}_\parallel(\mathbf{k}) \end{pmatrix}. \quad (2)$$

Here the k_z dependence only appears due to the phase factors, with d being the height of the bilayer sandwich. The hats are used to remind the reader that all blocks are, in principle, square matrices in the orbital degree of freedom. The above Hamiltonian can be block-diagonalized using the transformation

$$V = \frac{1}{\sqrt{2}} \begin{pmatrix} \mathbb{1} & \mathbb{1} e^{ik_zd} \\ \mathbb{1} e^{-ik_zd} & -\mathbb{1} \end{pmatrix}, \quad \hat{H}^{b/a} = \hat{H}_\parallel \pm \hat{H}_\perp, \quad (3)$$

where the blocks belong to the bonding (b) and antibonding (a) subspaces. Note that the phase factor is not present in the (ab) space.

For the interaction part of the Hamiltonian we include the on-site intraorbital (U) and interorbital (U'), Hund's type ($J_{\rm H}$), and pair hopping (J') interaction, and we assume spin-rotational invariance, which yields the relations $U' = U - 2J_{\rm H}$ and $J_{\rm H} = J'$ [16,89].

The noninteracting multiorbital susceptibility in the superconducting state can be written in terms of normal and anomalous Green's functions as

$$(\chi_0)^{\eta_2\eta_3}_{\eta_1\eta_4}(q) = \frac{T}{N}\sum_k [F_{\eta_1\eta_3}(k+q)\bar{F}_{\eta_2\eta_4}(k) - G_{\eta_1\eta_2}(k+q)G_{\eta_3\eta_4}(k)], \tag{4}$$

where we use the four notation $k = (\mathbf{k}, k_z, i\omega_n)$ and shorthand indices $\eta = (l, o, s)$. To compute the spin susceptibility, we use the random-phase approximation (RPA) [16,89]. The interacting susceptibility can be written as a matrix equation with susceptibility matrices of the form

$$\hat{\chi}(q_z) = \begin{pmatrix} \hat{\chi}_\parallel & \hat{\chi}_\perp e^{iq_zd} \\ \hat{\chi}_\perp e^{-iq_zd} & \hat{\chi}_\parallel \end{pmatrix}, \tag{5}$$

where we suppress the in-plane momentum dependence $\mathbf{q}$ and the dependence on Matsubara frequencies and the q_z dependence only enters via the phase factors. The Dyson-type RPA matrix equation can be decomposed into even and odd channels with respect to the exchange of layer index by defining $\hat{\chi}^{e/o} = 2(\hat{\chi}_\parallel \pm \hat{\chi}_\perp)$:

$$\hat{\chi}^{(e/o)} = \left[\mathbb{1} - \frac{1}{2}\hat{\chi}_0^{(e/o)}\hat{U}\right]^{-1}\hat{\chi}_0^{(e/o)}, \tag{6}$$

where χ_0 denotes the noninteracting susceptibilities. The above expression holds in general for both the spin and the charge susceptibilities, but the interaction matrix $\hat{U}$ has to be chosen differently. For the physical paramagnetic susceptibility we have to contract the orbital and sublattice degrees of freedom at the free vertices. In terms of $\hat{\chi}_e$ and $\hat{\chi}_o$, it can be written as

$$\chi_{\rm spin} = \sum_{l_1l_2,o_1o_2} \begin{pmatrix} \hat{\chi}^e + \hat{\chi}^o & (\hat{\chi}^e - \chi^o)e^{iq_zd} \\ (\hat{\chi}^e - \hat{\chi}^o)e^{-iq_zd} & \hat{\chi}^e + \hat{\chi}^o \end{pmatrix}_{l_1o_1;l_2o_2} = \sum_{o_1,o_2}\left[\hat{\chi}^e_{o_1,o_2}\cos^2\left(\frac{q_zd}{2}\right) + \hat{\chi}^o_{o_1,o_2}\sin^2\left(\frac{q_zd}{2}\right)\right]. \tag{7}$$

This expression of the spin susceptibility has been initially derived for the bilayer cuprates [76,82,85]. By explicitly using the matrix elements from Eq. (3), we can express the even and the odd susceptibilities through susceptibilities in the (ab) space: $\hat{\chi}^e_0 = \hat{\chi}^{aa} + \hat{\chi}^{bb}$ and $\hat{\chi}^o_0 = \hat{\chi}^{ab} + \hat{\chi}^{ba}$. For more information on the theoretical approach and the used parameters, see the Supplemental Material [90].

Results. In what follows we compute the bilayer spin response for pressurized $La_3Ni_2O_7$ for two slightly different tight-binding parametrizations of the noninteracting Hamiltonian to observe the general trends. In Figs. 1(c) and 1(e) and Fig. 3(c) we show the normal-state even and odd components of the bilayer spin susceptibility using the tight-binding model from Refs. [16,33], respectively. One immediately sees that, independent of the model used, the magnetic responses in the odd and the even channels strongly differ from each other with respect to the dominant scattering peaks. Specifically, the main scatterings in the even channel stem from the scattering within the antibonding β band and within the bonding γ band ($\mathbf{q}_1^e$ and $\mathbf{q}_2^e$), as well as from scattering between bonding α and γ bands ($\mathbf{q}_3^e$), which is illustrated in Fig. 1(b). At the same time, the main scatterings in the odd channel stem from scattering between bonding α band to antibonding β band ($\mathbf{q}_2^o$)

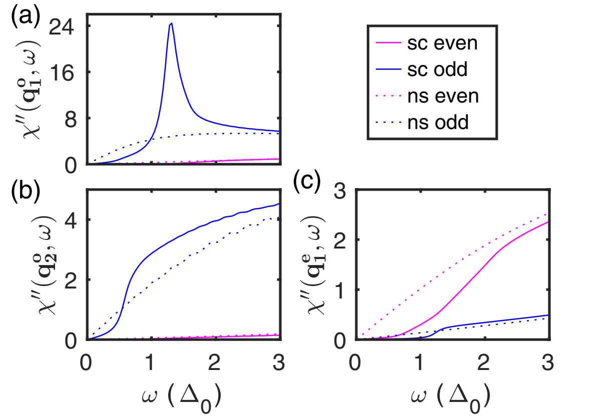

FIG. 2. Calculated frequency dependence of the imaginary part of the even and the odd spin susceptibility in the bonding-antibonding $s_\pm$-wave superconducting (solid curves) and normal (dashed curves) states using the tight-binding parameters from Ref. [33]. The representative wave vectors $\mathbf{q}_1^o$ (a), $\mathbf{q}_2^o$ (b), and $\mathbf{q}_1^e$ (c) are chosen from Fig. 1.

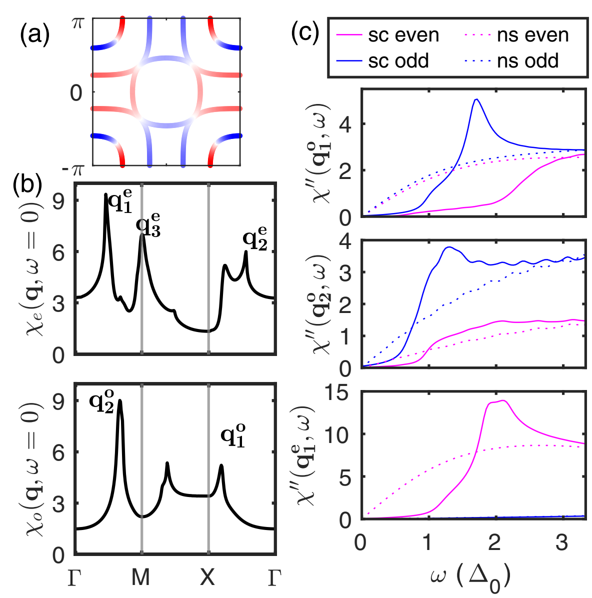

FIG. 3. (a) Sketch of the $d_{x^2-y^2}$-wave gap solution for the tight-binding model [16] where blue and red colors refer to the opposite signs of the gap magnitudes. Panel (b) shows the even (χ_e) and the odd (χ_o) parts of the static RPA susceptibility, respectively, calculated in the normal state ($T = 80$ K) for $U = 0.9U_{\rm mag}$ and $J_{\rm H} = U/4$. Panel (c) shows the calculated frequency dependence of the imaginary part at the characteristic maximal scattering wave vectors of the even and the odd spin susceptibility for the $d_{x^2-y^2}$-wave superconducting (solid curves) and normal (dashed curves) states and the maximum gap magnitude of $\Delta_0 = 15$ meV. Note that in the bottom panel the blue lines are near 0.

and bonding γ band to antibonding β band ($\mathbf{q}_1^o$), which is displayed in Fig. 1(d). Apart from different magnitudes, these peaks are dominant in both models. The different behavior in both channels arises from the large bonding-antibonding splitting of the electronic bands, as can be seen by looking at the noninteracting susceptibility presented in Fig. 1 of the Supplemental Material [90], and does not require the effective interlayer interaction.

Despite the similar $\mathbf{q}$ dependence of the spin response in both models, the dominant superconducting instabilities appear to be different. While models based on Ref. [33] and spin-fluctuation-mediated pairing mostly predict sign-changing bonding-antibonding s-wave solutions [18,19], similar spin-fluctuation-based analyses reveal d-wave symmetries to be present in the other model [16,17]. One can understand this difference by simply looking into the overall magnitudes of the even and odd susceptibilities. In the case of the tight-binding model of Ref. [33], the odd susceptibility appears to be twice larger in magnitude than the even susceptibility, which indicates the dominance of the interlayer itinerant magnetic fluctuations. This dominance of the magnetic fluctuations in the odd channel supports the interlayer (bonding-antibonding) $s_\pm$-wave Cooper pairing with large interlayer superconducting gap [36,38]. At the same time, within the other tight-binding model [16], the different peaks in the odd and the even susceptibilities appear to have similar magnitudes, and among several candidates, the d-wave superconducting gap appears to be the most stable solution. One should further note at this point that the d-wave symmetry is usually more stable against the inclusion of the local Coulomb interaction, and even in the case of near competition between various channels this solution usually wins [91].

The strong differentiation of the even and the odd susceptibilities seen in the normal state offer now a practical tool to disentangle between various Cooper-pairing scenarios. For this, we now extend the calculations of the spin response to the superconducting state by comparing the structure of the spin response for the model giving the sign-changing bonding-antibonding s-wave solution [33] and that which gives the d-wave solution to be the most dominant [16].

Note that the bonding-antibonding $s_\pm$-wave solution in the (ab) space allows for a simple decomposition of the Cooper-pairing to the interlayer and intralayer contribution. In particular, we can write the gaps in the sublattice space as $\hat{\Delta}^{a/b} = \hat{\Delta} \pm \hat{\Delta}^\perp$, where $\hat{\Delta}^\parallel$ and $\hat{\Delta}^\perp$ are the intralayer and the interlayer superconducting order parameters, respectively. By setting $\Delta^\perp_{x^2-y^2} = \Delta^\perp_{z^2}$ and $\hat{\Delta}^\parallel = 0$, one ends up with a constant magnitude gap, which, however, changes sign between bonding and antibonding bands. This gap symmetry is consistent with the numerical solutions found in the literature [16–27] and is illustrated in Fig. 1(b).

Given the peculiar structure of the sign-changing bonding-antibonding gap, the spin resonance in the spin susceptibility exclusively appears in the odd channel with the scattering between bonding and antibonding bands, but not in the even channel. In particular, we show in Fig. 2 the calculated frequency dependence of the imaginary parts of the even, $\mathrm{Im}\chi_e$, and the odd, $\mathrm{Im}\chi_o$, spin susceptibilities at the characteristic wave vectors $\mathbf{q}_1^o$, $\mathbf{q}_2^o$, and $\mathbf{q}_1^e$ identified in the normal state and employing the characteristic gap size of $\Delta_0 = 15$ meV, which yields a plausible gap-to-T_c ratio of about 4.3. Observe that the enhancement occurs only for the odd spin response at $\mathbf{q}_1^o$ and $\mathbf{q}_2^o$, where the superconducting gap changes sign between bonding and antibonding bands and the exact magnitude depends on the values of the superconducting gap at the corresponding region. On the contrary, the spin susceptibility in the even channel at $\mathbf{q}_1^e$ is suppressed as generally the scattering wave vectors within bonding or antibonding bands connect regions of the same gap sign of the superconducting order parameter. In this regard, the outlined behavior of the spin response, i.e., the enhancement of the odd spin susceptibility and its absence in the even channel in the experiment probed by inelastic neutron scattering or resonant inelastic x-ray scattering (RIXS) will be a direct probe for the interlayer Cooper pairing and bonding-antibonding character of the $s_\pm$-wave gap.

The obtained results are robust to small variations of the gap. The solutions discussed in the literature sometimes show nodal regions appearing in the Γ-M direction, which can be incorporated by fine-tuning and inclusion of interorbital gaps or by including the gaps directly in band space, which we have done for the results shown. However, we find that such details are essentially irrelevant for the generic behavior of the spin resonance. Three different $s_\pm$ gap functions are compared exemplarily in the Supplemental Material [90].

Let us now turn to the discussion of the spin response for the second of the models outlined in Ref. [16], which give the $d_{x^2-y^2}$-wave superconducting gap symmetry, shown in Fig. 3(a). Here we should mention that due to the mixed orbital character of the α band and the β band the $d_{x^2-y^2}$-wave solution cannot be straightforwardly decomposed in the orbital and sublattice degrees of freedom. Instead we introduce the gap function in the band space, and having in mind that it has different contributions, we include those from interorbital and inter- and intralayer gaps, which is required to avoid interband gaps.

In contrast to the bonding-antibonding $s_\pm$-wave scenario, a sizable enhancement of $\mathrm{Im}\chi$ in the d-wave superconducting state is seen in the odd channel at $\mathbf{q}_1^o$ as well as in the even channel near $\mathbf{q}_1^e$ as shown in Fig. 3(c). The differences in the overall magnitude can be traced back to the angular dependence of the superconducting gap at the Fermi surface. For example, there is no sign change of the gap on the β Fermi surface sheet portions for the wave vectors $\mathbf{q}_1^e$ and $\mathbf{q}_2^e$, shown as arrows in Fig. 1(b). In fact, it is the scattering across the γ pocket that causes the enhancement and happens to be peaked at the same momentum transfer. The large intraband contributions from the γ band to the susceptibility can be attributed to its flatness. In contrast to the odd spin resonance in the $s_\pm$-wave scenario, the resonances in the odd and even channels in the $d_{x^2-y^2}$-wave scenario are much broader and for the even channel are also strongly dispersing in the momentum space, which is shown in Fig. 2(b) of the Supplemental Material [90]. Most importantly, within the d-wave scenario there is no sizeable difference in the magnitude of the enhancements of the spin response in the superconducting state in the odd and the even channel.

Let us also mention that in Refs. [16,17,27] the d_{xy}-wave solution was also appearing as one of the leading instabilities for smaller Hund's coupling. Similar to the $d_{x^2-y^2}$ case, we find a sharp spin resonance peak in the odd channel at $\mathbf{q}_1^o$ and a broad peak in the even channel with the dispersion along Γ-X direction, which is shown in Fig. 2(c) of the Supplemental Material [90], while in the $d_{x^2-y^2}$ case one finds the dispersion along Γ-M direction. Therefore d_{xy} and $d_{x^2-y^2}$ pairing symmetries can be distinguished by comparing the Γ-X and Γ-M directions for the even channel of the spin susceptibility.

A different Fermi surface topology in which the γ pocket sinks below the Fermi surface has been predicted in Ref. [29], which is in line with the recent angle-resolved photoemission spectroscopy results for ambient pressure [92]. For the bonding-antibonding $s_{\pm}$-wave Cooper-pairing scenario, which changes sign between α and β bands, a spin resonance would appear exclusively at $\mathbf{q}_2^o$. The scattering vector $\mathbf{q}_2^o$ may also play an important role in the magnetic ordering at ambient pressure. In the reciprocal space index corresponding to the pseudotetragonal unit cell (H, K, L), this peak is located at $(0.34, 0.34, c/(2d) \approx 2.6)$ close to the magnetic peak (0.25, 0.25, 2.5) found in very recent RIXS measurements at ambient pressure [93]. We believe that the fact that in experiment this peak was found to be nondispersive but losing intensity away from $L = 2.5$ towards lower L (see Fig. 2(c) in Ref. [93]) is an indicator of being present in the odd channel exclusively.

Conclusion. We have shown that the interlayer bonding-antibonding $s_{\pm}$ and d-wave pairing scenarios yield clearly distinguishable bilayer spin responses in the normal and the superconducting states. The $s_{\pm}$-wave Cooper pairing gives rise to a strong spin resonance peak in the odd channel of the spin susceptibility, whereas the even response shows no enhancement. In contrast, for the d-wave symmetry, spin-resonancelike weaker peaks appear in both even and odd channels. Therefore, studying bilayer structure of the spin response in the $La_3Ni_2O_7$ may provide a crucial check for the superconducting gap symmetry.

Acknowledgment. The work is supported by the German Research Foundation within the bilateral NSFC-DFG Project ER 463/14-1.

[1] D. Li, K. Lee, B. Y. Wang, M. Osada, S. Crossley, H. R. Lee, Y. Cui, Y. Hikita, and H. Y. Hwang, Superconductivity in an infinite-layer nickelate, Nature (London) **572**, 624 (2019).

[2] G. A. Pan, D. Ferenc Segedin, H. LaBollita, Q. Song, E. M. Nica, B. H. Goodge, A. T. Pierce, S. Doyle, S. Novakov, D. C. Carrizales, A. T. N'Diaye, P. Shafer, H. Paik, J. T. Heron, J. A. Mason, A. Yacoby, L. F. Kourkoutis, O. Erten, C. M. Brooks, A. S. Botana *et al.*, Superconductivity in a quintuple-layer square-planar nickelate, Nat. Mater. **21**, 160 (2022).

[3] M. Osada, B. Y. Wang, B. H. Goodge, K. Lee, H. Yoon, K. Sakuma, D. Li, M. Miura, L. F. Kourkoutis, and H. Y. Hwang, A superconducting praseodymium nickelate with infinite layer structure, Nano Lett. **20**, 5735 (2020).

[4] H. Sun, M. Huo, X. Hu, J. Li, Z. Liu, Y. Han, L. Tang, Z. Mao, P. Yang, B. Wang, J. Cheng, D.-X. Yao, G.-M. Zhang, and M. Wang, Signatures of superconductivity near 80 K in a nickelate under high pressure, Nature (London) **621**, 493 (2023).

[5] J. Hou, P.-T. Yang, Z.-Y. Liu, J.-Y. Li, P.-F. Shan, L. Ma, G. Wang, N.-N. Wang, H.-Z. Guo, J.-P. Sun, Y. Uwatoko, M. Wang, G.-M. Zhang, B.-S. Wang, and J.-G. Cheng, Emergence of high-temperature superconducting phase in pressurized $La_3Ni_2O_7$ crystals, Chin. Phys. Lett. **40**, 117302 (2023).

[6] Y. Zhang, D. Su, Y. Huang, H. Sun, M. Huo, Z. Shan, K. Ye, Z. Yang, R. Li, M. Smidman, M. Wang, L. Jiao, and H. Yuan, High-temperature superconductivity with zero-resistance and strange metal behavior in $La_3Ni_2O_{7-\delta}$, arXiv:2307.14819.

[7] Y. Zhou, J. Guo, S. Cai, H. Sun, P. Wang, J. Zhao, J. Han, X. Chen, Q. Wu, Y. Ding, M. Wang, T. Xiang, H.-kwang Mao, and L. Sun, Evidence of filamentary superconductivity in pressurized $La_3Ni_2O_7$ single crystals, arXiv:2311.12361.

[8] M. Zhang, C. Pei, Q. Wang, Y. Zhao, C. Li, W. Cao, S. Zhu, J. Wu, and Y. Qi, Effects of pressure and doping on Ruddlesden-Popper phases $La_{n+1}Ni_nO_{3n+1}$, J. Mater. Sci. Technol. **185**, 147 (2024).

[9] L. Wang, Y. Li, S. Xie, F. Liu, H. Sun, C. Huang, Y. Gao, T. Nakagawa, B. Fu, B. Dong, Z. Cao, R. Yu, S. I. Kawaguchi, H. Kadobayashi, M. Wang, C. Jin, H.-k. Mao, and H. Liu, Structure responsible for the superconducting state in $La_3Ni_2O_7$ at low temperature and high pressure conditions, arXiv:2311.09186.

[10] G. Wang, N. N. Wang, X. L. Shen, J. Hou, L. Ma, L. F. Shi, Z. A. Ren, Y. D. Gu, H. M. Ma, P. T. Yang, Z. Y. Liu, H. Z. Guo, J. P. Sun, G. M. Zhang, S. Calder, J.-Q. Yan, B. S. Wang, Y. Uwatoko, and J.-G. Cheng, Pressure-induced superconductivity in polycrystalline $La_3Ni_2O_{7-\delta}$, Phys. Rev. X **14**, 011040 (2024).

[11] Z. Dong, M. Huo, J. Li, J. Li, P. Li, H. Sun, Y. Lu, M. Wang, Y. Wang, and Z. Chen, Visualization of oxygen vacancies and self-doped ligand holes in $La_3Ni_2O_{7-\delta}$, arXiv:2312.15727.

[12] H. Sakakibara, M. Ochi, H. Nagata, Y. Ueki, H. Sakurai, R. Matsumoto, K. Terashima, K. Hirose, H. Ohta, M. Kato, Y. Takano, and K. Kuroki, Theoretical analysis on the possibility of superconductivity in a trilayer Ruddlesden-Popper nickelate $La_4Ni_3O_{10}$ under pressure and its experimental examination: Comparison with $La_3Ni_2O_7$, Phys. Rev. B **109**, 144511 (2024).

[13] Q. Li, Y.-J. Zhang, Z.-N. Xiang, Y. Zhang, X. Zhu, and H.-H. Wen, Signature of superconductivity in pressurized $La_4Ni_3O_{10}$, Chin. Phys. Lett. **41**, 017401 (2024).

[14] M. Zhang, C. Pei, X. Du, Y. Cao, Q. Wang, J. Wu, Y. Li, Y. Zhao, C. Li, W. Cao, S. Zhu, Q. Zhang, N. Yu, P. Cheng, J. Zhao, Y. Chen, H. Guo, L. Yang, and Y. Qi, Superconductivity in trilayer nickelate $La_4Ni_3O_{10}$ under pressure, arXiv:2311.07423.

[15] Y. Zhu, E. Zhang, B. Pan, X. Chen, D. Peng, L. Chen, H. Ren, F. Liu, N. Li, Z. Xing, J. Han, J. Wang, D. Jia, H. Wo, Y. Gu, Y. Gu, L. Ji, W. Wang, H. Gou, Y. Shen *et al.*, Superconductivity in trilayer nickelate $La_4Ni_3O_{10}$ single crystals, arXiv:2311.07353.

[16] F. Lechermann, J. Gondolf, S. Bötzel, and I. M. Eremin, Electronic correlations and superconducting instability in $La_3Ni_2O_7$ under high pressure, Phys. Rev. B **108**, L201121 (2023).

[17] H. Liu, C. Xia, S. Zhou, and H. Chen, Role of crystal-field-splitting and longe-range-hoppings on superconducting pairing symmetry of $La_3Ni_2O_7$, arXiv:2311.07316.

[18] H. Oh and Y.-H. Zhang, Type-II $t - J$ model and shared superexchange coupling from Hund's rule in superconducting $La_3Ni_2O_7$, Phys. Rev. B **108**, 174511 (2023).

[19] Z. Luo, B. Lv, M. Wang, W. Wú, and D.-x. Yao, High-T_C superconductivity in $La_3Ni_2O_7$ based on the bilayer two-orbital t-J model, arXiv:2308.16564.
[20] Q. Qin and Y.-f. Yang, High-T_c superconductivity by mobilizing local spin singlets and possible route to higher T_c in pressurized $La_3Ni_2O_7$, Phys. Rev. B **108**, L140504 (2023).
[21] J. Huang, Z. D. Wang, and T. Zhou, Impurity and vortex states in the bilayer high-temperature superconductor $La_3Ni_2O_7$, Phys. Rev. B **108**, 174501 (2023).
[22] X.-Z. Qu, D.-W. Qu, J. Chen, C. Wu, F. Yang, W. Li, and G. Su, Bilayer t-J-$J_\perp$ model and magnetically mediated pairing in the pressurized nickelate $La_3Ni_2O_7$, Phys. Rev. Lett. **132**, 036502 (2024).
[23] Y. Zhang, L.-F. Lin, A. Moreo, T. A. Maier, and E. Dagotto, Trends in electronic structures and $s_\pm$-wave pairing for the rare-earth series in bilayer nickelate superconductor $R_3Ni_2O_7$, Phys. Rev. B **108**, 165141 (2023).
[24] Q.-G. Yang, D. Wang, and Q.-H. Wang, Possible $s_\pm$-wave superconductivity in $La_3Ni_2O_7$, Phys. Rev. B **108**, L140505 (2023).
[25] Y. Zhang, L.-F. Lin, A. Moreo, T. A. Maier, and E. Dagotto, Structural phase transition, $s_\pm$-wave pairing, and magnetic stripe order in bilayered superconductor $La_3Ni_2O_7$ under pressure, Nat. Commun. **15**, 2470 (2024).
[26] H. Yang, H. Oh, and Y.-H. Zhang, Strong pairing from doping-induced Feshbach resonance and second Fermi liquid through doping a bilayer spin-one Mott insulator: Application to $La_3Ni_2O_7$, arXiv:2309.15095.
[27] G. Heier, K. Park, and S. Y. Savrasov, Competing d_{xy} and $s_\pm$ pairing symmetries in superconducting $La_3Ni_2O_7$: LDA + FLEX calculations, Phys. Rev. B **109**, 104508 (2024).
[28] K. Jiang, Z. Wang, and F.-C. Zhang, High-temperature superconductivity in $La_3Ni_2O_7$, Chin. Phys. Lett. **41**, 017402 (2023).
[29] S. Ryee, N. Witt, and T. O. Wehling, Critical role of interlayer dimer correlations in the superconductivity of $La_3Ni_2O_7$, arXiv:2310.17465.
[30] Y.-H. Tian, Y. Chen, J.-M. Wang, R.-Q. He, and Z.-Y. Lu, Correlation effects and concomitant two-orbital $s_\pm$-wave superconductivity in la $La_3Ni_2O_7$ under high pressure, arXiv:2308.09698.
[31] Z. Liao, L. Chen, G. Duan, Y. Wang, C. Liu, R. Yu, and Q. Si, Electron correlations and superconductivity in $La_3Ni_2O_7$ under pressure tuning, arXiv:2307.16697.
[32] T. Kaneko, H. Sakakibara, M. Ochi, and K. Kuroki, Pair correlations in the two-orbital Hubbard ladder: Implications for superconductivity in the bilayer nickelate $La_3Ni_2O_7$, Phys. Rev. B **109**, 045154 (2024).
[33] Z. Luo, X. Hu, M. Wang, W. Wú, and D.-X. Yao, Bilayer two-orbital model of $La_3Ni_2O_7$ under pressure, Phys. Rev. Lett. **131**, 126001 (2023).
[34] J. Chen, F. Yang, and W. Li, Orbital-selective superconductivity in the pressurized bilayer nickelate $La_3Ni_2O_7$: An infinite projected entangled-pair state study, arXiv:2311.05491.
[35] Y. Shen, M. Qin, and G.-M. Zhang, Effective bi-layer model Hamiltonian and density-matrix renormalization group study for the high-T_c superconductivity in $La_3Ni_2O_7$ under high pressure, Chin. Phys. Lett. **40**, 127401 (2023).
[36] Y.-f. Yang, G.-M. Zhang, and F.-C. Zhang, Interlayer valence bonds and two-component theory for high-T_c superconductivity of $La_3Ni_2O_7$ under pressure, Phys. Rev. B **108**, L201108 (2023).
[37] W. Wú, Z. Luo, D.-X. Yao, and M. Wang, Superexchange and charge transfer in the nickelate superconductor $La_3Ni_2O_7$ under pressure, Sci. China: Phys., Mech. Astron. **67**, 117402 (2024).
[38] C. Lu, Z. Pan, F. Yang, and C. Wu, Interplay of two E_g orbitals in superconducting $La_3Ni_2O_7$ under pressure, arXiv:2310.02915.
[39] D. A. Shilenko and I. V. Leonov, Correlated electronic structure, orbital-selective behavior, and magnetic correlations in double-layer $La_3Ni_2O_7$ under pressure, Phys. Rev. B **108**, 125105 (2023).
[40] Y. Zhang, L.-F. Lin, A. Moreo, and E. Dagotto, Electronic structure, dimer physics, orbital-selective behavior, and magnetic tendencies in the bilayer nickelate superconductor $La_3Ni_2O_7$ under pressure, Phys. Rev. B **108**, L180510 (2023).
[41] B. Geisler, J. J. Hamlin, G. R. Stewart, R. G. Hennig, and P. Hirschfeld, Structural transitions, octahedral rotations, and electronic properties of $A_3Ni_2O_7$ rare-earth nickelates under high pressure, arXiv:2309.15078.
[42] H. Lange, L. Homeier, E. Demler, U. Schollwöck, F. Grusdt, and A. Bohrdt, Feshbach resonance in a strongly repulsive bilayer model: a possible scenario for bilayer nickelate superconductors, arXiv:2309.15843.
[43] H. LaBollita, V. Pardo, M. R. Norman, and A. S. Botana, Electronic structure and magnetic properties of $La_3Ni_2O_7$ under pressure: active role of the Ni-$d_{x^2-y^2}$ orbitals, arXiv:2309.17279.
[44] L. C. Rhodes and P. Wahl, Structural routes to stabilise superconducting $La_3Ni_2O_7$ at ambient pressure, Phys. Rev. Mater. **8**, 044801 (2024).
[45] J.-X. Zhang, H.-K. Zhang, Y.-Z. You, and Z.-Y. Weng, Strong pairing originated from an emergent $\mathbb{Z}_2$ Berry phase in $La_3Ni_2O_7$, arXiv:2309.05726.
[46] C. Lu, Z. Pan, F. Yang, and C. Wu, Interlayer-coupling-driven high-temperature superconductivity in $La_3Ni_2O_7$ under pressure, Phys. Rev. Lett. **132**, 146002 (2024).
[47] X. Chen, P. Jiang, J. Li, Z. Zhong, and Y. Lu, Critical charge and spin instabilities in superconducting $La_3Ni_2O_7$, arXiv:2307.07154.
[48] Y. Cao and Y.-f. Yang, Flat bands promoted by Hund's rule coupling in the candidate double-layer high-temperature superconductor $La_3Ni_2O_7$ under high pressure, Phys. Rev. B **109**, L081105 (2024).
[49] V. Christiansson, F. Petocchi, and P. Werner, Correlated electronic structure of $La_3Ni_2O_7$ under pressure, Phys. Rev. Lett. **131**, 206501 (2023).
[50] Y.-Y. Zheng and W. Wú, Superconductivity in the bilayer two-orbital Hubbard model, arXiv:2312.03605.
[51] M. Kakoi, T. Kaneko, H. Sakakibara, M. Ochi, and K. Kuroki, Pair correlations of the hybridized orbitals in a ladder model for the bilayer nickelate $La_3Ni_2O_7$, arXiv:2312.04304.
[52] Z. Fan, J.-F. Zhang, B. Zhan, D. Lv, X.-Y. Jiang, B. Normand, and T. Xiang, Superconductivity in nickelate and cuprate superconductors with strong bilayer coupling, arXiv:2312.17064.
[53] B. Geisler, L. Fanfarillo, J. J. Hamlin, G. R. Stewart, R. G. Hennig, and P. J. Hirschfeld, Optical properties and electronic correlations in $La_3Ni_2O_{7-\delta}$ bilayer nickelates under high pressure, arXiv:2401.04258.
[54] H. Sakakibara, N. Kitamine, M. Ochi, and K. Kuroki, Possible high T_c superconductivity in $La_3Ni_2O_7$ under high pressure

through manifestation of a nearly half-filled bilayer Hubbard model, Phys. Rev. Lett. **132**, 106002 (2024).

[55] P. Puphal, P. Reiss, N. Enderlein, Y.-M. Wu, G. Khaliullin, V. Sundaramurthy, T. Priessnitz, M. Knauft, L. Richter, M. Isobe, P. A. van Aken, H. Takagi, B. Keimer, Y. E. Suyolcu, B. Wehinger, P. Hansmann, and M. Hepting, Unconventional crystal structure of the high-pressure superconductor $La_3Ni_2O_7$, arXiv:2312.07341.

[56] X. Chen, J. Zhang, A. S. Thind, S. Sharma, H. LaBollita, G. Peterson, H. Zheng, D. P. Phelan, A. S. Botana, R. F. Klie, and J. F. Mitchell, Polymorphism in the Ruddlesden-Popper nickelate $La_3Ni_2O_7$: Discovery of a hidden phase with distinctive layer stacking, J. Am. Chem. Soc. **146**, 3640 (2024).

[57] E. Dagotto, J. Riera, and D. Scalapino, Superconductivity in ladders and coupled planes, Phys. Rev. B **45**, 5744 (1992).

[58] K. Chen, X. Liu, J. Jiao, M. Zou, Y. Luo, Q. Wu, N. Zhang, Y. Guo, and L. Shu, Evidence of spin density waves in $La_3Ni_2O_{7-\delta}$, arXiv:2311.15717.

[59] Z. Liu, H. Sun, M. Huo, X. Ma, Y. Ji, E. Yi, L. Li, H. Liu, J. Yu, Z. Zhang *et al.*, Evidence for charge and spin density waves in single crystals of $La_3Ni_2O_7$ and $La_3Ni_2O_6$, Sci. China: Phys., Mech. Astron. **66**, 217411 (2023).

[60] G. Yu, Y. Li, E. Motoyama, and M. Greven, A universal relationship between magnetic resonance and superconducting gap in unconventional superconductors, Nat. Phys. **5**, 873 (2009).

[61] J. Rossat-Mignod, L. Regnault, C. Vettier, P. Bourges, P. Burlet, J. Bossy, J. Henry, and G. Lapertot, Neutron scattering study of the $YBa_2Cu_3O_{6+x}$ system, Phys. C (Amsterdam, Neth.) **185-189**, 86 (1991).

[62] H. A. Mook, M. Yethiraj, G. Aeppli, T. E. Mason, and T. Armstrong, Polarized neutron determination of the magnetic excitations in $YBa_2Cu_3O_7$, Phys. Rev. Lett. **70**, 3490 (1993).

[63] P. Bourges, L. P. Regnault, Y. Sidis, and C. Vettier, Inelastic-neutron-scattering study of antiferromagnetic fluctuations in $YBa_2Cu_3O_{6.97}$, Phys. Rev. B **53**, 876 (1996).

[64] P. Dai, H. A. Mook, S. M. Hayden, G. Aeppli, T. G. Perring, R. D. Hunt, and F. Doğan, The magnetic excitation spectrum and thermodynamics of high-T_c superconductors, Science **284**, 1344 (1999).

[65] V. Hinkov, P. Bourges, S. Pailhès, Y. Sidis, A. Ivanov, C. D. Frost, T. G. Perring, C. T. Lin, D. P. Chen, and B. Keimer, Spin dynamics in the pseudogap state of a high-temperature superconductor, Nat. Phys. **3**, 780 (2007).

[66] A. D. Christianson, E. A. Goremychkin, R. Osborn, S. Rosenkranz, M. D. Lumsden, C. D. Malliakas, I. S. Todorov, H. Claus, D. Y. Chung, M. G. Kanatzidis, R. I. Bewley, and T. Guidi, Unconventional superconductivity in $Ba_{0.6}K_{0.4}Fe_2As_2$ from inelastic neutron scattering, Nature (London) **456**, 930 (2008).

[67] D. S. Inosov, J. T. Park, P. Bourges, D. L. Sun, Y. Sidis, A. Schneidewind, K. Hradil, D. Haug, C. T. Lin, B. Keimer, and V. Hinkov, Normal-state spin dynamics and temperature-dependent spin-resonance energy in optimally doped $BaFe_{1.85}Co_{0.15}As_2$, Nat. Phys. **6**, 178 (2010).

[68] J. T. Park, G. Friemel, Y. Li, J.-H. Kim, V. Tsurkan, J. Deisenhofer, H.-A. Krug von Nidda, A. Loidl, A. Ivanov, B. Keimer, and D. S. Inosov, Magnetic resonant mode in the low-energy spin-excitation spectrum of superconducting $Rb_2Fe_4Se_5$ single crystals, Phys. Rev. Lett. **107**, 177005 (2011).

[69] P. Dai, Antiferromagnetic order and spin dynamics in iron-based superconductors, Rev. Mod. Phys. **87**, 855 (2015).

[70] C. Stock, C. Broholm, J. Hudis, H. J. Kang, and C. Petrovic, Spin resonance in the d-wave superconductor $CeCoIn_5$, Phys. Rev. Lett. **100**, 087001 (2008).

[71] Y. Song, W. Wang, J. S. Van Dyke, N. Pouse, S. Ran, D. Yazici, A. Schneidewind, P. Čermák, Y. Qiu, M. B. Maple, D. K. Morr, and P. Dai, Nature of the spin resonance mode in $CeColn_5$, Commun. Phys. **3**, 98 (2020).

[72] D. J. Scalapino, A common thread: The pairing interaction for unconventional superconductors, Rev. Mod. Phys. **84**, 1383 (2012).

[73] N. Bulut, D. J. Scalapino, and R. T. Scalettar, Nodeless d-wave pairing in a two-layer Hubbard model, Phys. Rev. B **45**, 5577 (1992).

[74] H. F. Fong, B. Keimer, P. W. Anderson, D. Reznik, F. Doğan, and I. A. Aksay, Phonon and magnetic neutron scattering at 41 meV in $YBa_2Cu_3O_7$, Phys. Rev. Lett. **75**, 316 (1995).

[75] A. Abanov and A. V. Chubukov, A relation between the resonance neutron peak and ARPES data in cuprates, Phys. Rev. Lett. **83**, 1652 (1999).

[76] J. Brinckmann and P. A. Lee, Slave boson approach to neutron scattering in $YBa_2Cu_3O_{6+y}$ superconductors, Phys. Rev. Lett. **82**, 2915 (1999).

[77] M. R. Norman, Relation of neutron incommensurability to electronic structure in high-temperature superconductors, Phys. Rev. B **61**, 14751 (2000).

[78] Y.-J. Kao, Q. Si, and K. Levin, Frequency evolution of neutron peaks below T_c: Commensurate and incommensurate structure in $La_{0.85}Sr_{0.15}CuO_4$ and $YBa_2Cu_3O_{6.6}$, Phys. Rev. B **61**, R11898 (2000).

[79] A. V. Chubukov, B. Jankó, and O. Tchernyshyov, Dispersion of the neutron resonance in cuprate superconductors, Phys. Rev. B **63**, 180507(R) (2001).

[80] F. Onufrieva and P. Pfeuty, Spin dynamics of a two-dimensional metal in a superconducting state: Application to the high-T_c cuprates, Phys. Rev. B **65**, 054515 (2002).

[81] I. Eremin, D. K. Morr, A. V. Chubukov, K. H. Bennemann, and M. R. Norman, Novel neutron resonance mode in $d_{x^2-y^2}$-wave superconductors, Phys. Rev. Lett. **94**, 147001 (2005).

[82] M. Sato, S. Shamoto, J. M. Tranquada, G. Shirane, and B. Keimer, Two-dimensional antiferromagnetic excitations from a large single crystal of $YBa_2Cu_3O_{6.2}$, Phys. Rev. Lett. **61**, 1317 (1988).

[83] G. Blumberg, B. P. Stojković, and M. V. Klein, Antiferromagnetic excitations and van Hove singularities in $YBa_2Cu_3O_{6+x}$, Phys. Rev. B **52**, R15741(R) (1995).

[84] B. Normand, H. Kohno, and H. Fukuyama, Dynamic susceptibility and phonon anomalies in the bilayer t-J model, J. Phys. Soc. Jpn. **64**, 3903 (1995).

[85] I. Eremin, D. K. Morr, A. V. Chubukov, and K. Bennemann, Spin susceptibility in bilayered cuprates: Resonant magnetic excitations, Phys. Rev. B **75**, 184534 (2007).

[86] N. S. Headings, S. M. Hayden, J. Kulda, N. H. Babu, and D. A. Cardwell, Spin anisotropy of the magnetic excitations in the normal and superconducting states of optimally doped $YBa_2Cu_3O_{6.9}$ studied by polarized neutron spectroscopy, Phys. Rev. B **84**, 104513 (2011).

[87] S. Pailhès, C. Ulrich, B. Fauqué, V. Hinkov, Y. Sidis, A. Ivanov, C. T. Lin, B. Keimer, and P. Bourges, Doping dependence

of bilayer resonant spin excitations in $YCaBa_2Cu_3O_{6+x}$, Phys. Rev. Lett. **96**, 257001 (2006).
[88] L. Capogna, B. Fauqué, Y. Sidis, C. Ulrich, P. Bourges, S. Pailhès, A. Ivanov, J. L. Tallon, B. Liang, C. T. Lin, A. I. Rykov, and B. Keimer, Odd and even magnetic resonant modes in highly overdoped $Bi_2Sr_2CaCu_2O_{8+\delta}$, Phys. Rev. B **75**, 060502(R) (2007).
[89] S. Graser, T. Maier, P. Hirschfeld, and D. Scalapino, Near-degeneracy of several pairing channels in multiorbital models for the Fe pnictides, New J. Phys. **11**, 025016 (2009).
[90] See Supplemental Material at http://link.aps.org/supplemental/10.1103/PhysRevB.109.L180502 for additional information on the performed calculation of the spin susceptibility in the normal and the superconducting states, a detailed comparison of the spin resonances for the $d_{x^2-y^2}$-wave and the d_{xy}-wave gap functions, and a comparison for altered $s_{\pm}$-wave gap functions to demonstrate the robustness of the results, which also includes Ref. [94].
[91] E. J. König and P. Coleman, Coulomb problem in iron-based superconductors, Phys. Rev. B **99**, 144522 (2019).
[92] J. Yang, H. Sun, X. Hu, Y. Xie, T. Miao, H. Luo, H. Chen, B. Liang, W. Zhu, G. Qu *et al.*, Orbital-dependent electron correlation in double-layer nickelate $La_3Ni_2O_7$, arXiv:2309.01148.
[93] X. Chen, J. Choi, Z. Jiang, J. Mei, K. Jiang, J. Li, S. Agrestini, M. Garcia-Fernandez, X. Huang, H. Sun, D. Shen, M. Wang, J. Hu, Y. Lu, K.-J. Zhou, and D. Feng, Electronic and magnetic excitations in $La_3Ni_2O_7$, arXiv:2401.12657.
[94] W. Setyawan and S. Curtarolo, High-throughput electronic band structure calculations: Challenges and tools, Comput. Mater. Sci. **49**, 299 (2010).